Organ-wide and ploidy-dependent regulations both contribute to cell size determination: evidence from a computational model of tomato fruit

Valentina Baldazzi, Pierre Valsesia, Michel Génard, Nadia Bertin

Organ-wide and ploidy-dependent regulations both contribute to cell size determination: evidence from a computational model of tomato fruit

Valentina Baldazzi[123], Pierre Valsesia[1], Michel Génard[1], Nadia Bertin[1]

[1]INRA, PSH, France
[2]Université Côte d'Azur, INRA, CNRS, ISA, France
[3] Université Côte d'Azur, Inria, INRA, CNRS, UPMC Univ Paris 06, BIOCORE, France

Abstract

The development of a new organ is the result of coordinated events of cell division and expansion, in strong interaction with each other. This paper presents a dynamic model of tomato fruit development that includes cells division, endoreduplication and expansion processes. The model is used to investigate the interaction among these developmental processes, in the perspective of a neo-cellular theory. In particular, different control schemes (either cell-autonomous or organ-controlled) are tested and results compared to observed data from two contrasted genotypes. The model shows that a pure cell-autonomous control fails to reproduce the observed cell size distribution, and an organ-wide control is required in order to get realistic cell sizes. The model also supports the role of endoreduplication as an important determinant of the final cell size and suggests a possible interaction through carbon allocation and metabolism.

Keywords: cell size, division, development, expansion, endoreduplication, growth, model, ploidy, tomato

INTRODUCTION

Understanding the mechanisms underpinning fruit development from its early stages is of primary importance for biology and agronomy. Indeed, early stages are highly sensitive to biotic and abiotic stresses, with important

consequences on fruit set and yield. The development of a new organ is the result of coordinated events of cell division and expansion. Fruit growth starts immediately after pollination with intensive cell division. As development proceeds, the proliferative activity of cells progressively slows down giving way to a phase of pure cell enlargement during fruit growth and ripening. In many species, including tomato, the transition from cell division to expansion phases is accompanied by repeated DNA duplications without mitosis, a process called endoreduplication. The exact role of endoreduplication is still unclear. A strong correlation between cell ploidy (i.e number of DNA copies) and final cell size has been observed in different species (Bertin, 2005; Lee et al., 2007; Melaragno et al., 1993; Rewers et al., 2009), suggesting a role of endoreduplication into the control of organ growth (Breuer et al., 2010; Chevalier et al., 2011).

Understanding the way cell division, endoreduplication and expansion processes interact is crucial to predict the emergence of important morphological traits (fruit size, mass, shape and texture) and their dependence on environmental and genetic factors. Historically, a big debate has opposed two contrasting views, the cellular vs the organismal theory that set the control of organ growth at the level of the individual cell or of the whole tissue, respectively (reviewed in (Beemster et al., 2003; Fleming, 2006; John and Qi, 2008). In the recent years, a consensus view, the neo-cellular theory, has eventually emerged. Accordingly, although individual cells are the units of plant morphology, their behavior (division, expansion) is not autonomous, but coordinated at the organ level by cell-to-cell communication mechanisms, thus creating an effective interaction between cellular and whole-organ behavior (Beemster et al., 2003; Sablowski and Carnier Dornelas, 2014; Tsukaya, 2003). The existence of non-cell autonomous control of organ development has been demonstrated in Arabidopsis leaf (Kawade et al., 2010) but the underlying modes of action remain unclear and often system-specific (Ferjani et al., 2007; Han et al., 2014; Horiguchi and Tsukaya, 2011; Norman et al., 2011; Okello et al., 2015).

Computational models offer a unique tool to express and test biological hypotheses, in a well-defined and controlled manner. Not surprisingly, indeed, computational modeling has been largely used to investigate the relationships between organ development and the underlying cellular processes. Many works have addressed the question of organogenesis, relating local morphogenetic rules and cell mechanical properties with the emerging patterns near the meristem (Boudon et al., 2015; Dupuy et al., 2010; Kuchen et al., 2012; Löfke et al., 2015; Lucas et al., 2013; Robinson et al., 2011) (von Wangenheim et al., 2016). At the tissue scale, a few models have addressed the issue of cell's size variance based on observed kinematic patterns of cell division or growth rates, with a particular attention to the intrinsic stochasticity of cell-cycle related processes (Asl et al., 2011; Kawade and Tsukaya, 2017; Roeder et al., 2010). In most of these models, cell expansion is simply described via an average growth rate, possibly modulated by the ploidy level of the cell, without any reference to the underlying molecular mechanisms or to the environmental conditions.

To our knowledge, very few attempts have been made to explicitly model the interaction among cell division, expansion and endoreduplication from first principles and at the scale of organ development. In Fanwoua et al., 2013 a model of tomato fruit development have been developed that integrates cell division, expansion and endoreduplication processes based on a set of biologically-inspired rules. The fruit is described by a set of q classes of cells with the same age, ploidy and mass. Within each class, cell division and endoreduplication are described as discrete events that take place within a well-defined window of time, whenever a specific mass-to-ploidy threshold is reached. Cell growth in dry mass is modeled following a source-sink approach as a function of the thermal time, the cell ploidy-level and the external resources. The model is able to qualitatively capture the effect of environmental conditions (temperature, fruit load) on the final fruit dry mass, but hypotheses and parameters are hard to validate as comparaison to experimental data is lacking. Moreover, the water content of the cell is not considered preventing the analysis

of cell volumes.

Baldazzi and coworkers developed an integrated model of tomato fruit development which explicitly accounts for the dynamics of cell proliferation as well as for the mechanisms of cell expansion, in both dry and fresh masses, based on biophysical and thermodynamical principles (Baldazzi et al., 2012, 2013). Here, a new version of this model, which includes cell endoreduplication, is proposed. The model was used to investigate different hypotheses concerning the regulation and the interaction among cellular processes, with special attention to 1) the importance of an organ-wide regulation on cell growth and 2) the mechanisms of interaction between endoreduplication and cell expansion processes.

We focus on a natural, wild type organ development and we analyze the effect of organ-wide or cell ploidy-dependent regulation onto the dynamics of cell expansion. To this aim, different control schemes (either cell-autonomous or organ-controlled, with or without ploidy effect on cell expansion) were tested *in silico* by means of specific model variants. Simulation results were analyzed and compared to cell size distributions observed on two contrasted genotypes, a cherry and a large-fruited tomato variety.

The model shows that a pure cell-based control cannot reproduce the observed cell size distribution, and an organ-wide control is required in order to get realistic cell and fruit sizes. The model also supports the role of endoreduplication as an important modulator of the cell expansion potential, although the strength of this interaction might be genotype-specific. In particular, results suggest a likely interaction through carbon allocation and metabolism.

MATERIALS AND METHODS

Experimental data

Two datasets were collected from two glasshouse experiments performed at

INRA Avignon (south of France) in 2004 and 2007 on large-fruited (cv Levovil) and cherry (cv. Cervil) tomato genotypes of *Solanum lycospersicum* L.

The 2004 experiment fruits were collected from April to May (planting in February) whereas in the 2007 experiment fruits were sampled from October to December (planting in August). Plants were grown according to standard cultural practices. Trusses were pruned in order to homogenise truss size along the stem within each genotype. Maximum number of flowers left on each inflorescence was 12 for Cervil and 6 for Levovil. Flowers were pollinated by bumblebees. Air temperature and humidity were recorded hourly in each experiment and input in the model as external signals.

Flower buds and fruits were sampled at different time points relative to the time of flower anthesis (full-flower opening). Fruit fresh and dry mass and pericarp fresh mass were systematically measured at all times points, before further measurements. In 2004, half of the fruit pericarps were then analyzed by flow cytometry and the other half were used for the determination of cell number. The number of pericarp cells was measured after tissue dissociation according to a method adapted from that of Bünger-Kibler and Bangerth, 1982 and detailed in (Bertin et al., 2003). Cells were counted in aliquots of the cell suspension under an optical microscope, using Fuchs-Rosenthal chambers or Bürker chambers for the large and small fruits, respectively. Six to 8 aliquots per fruits were observed and the whole pericarp cell number was calculated according to dilution and observation volumes. The ploidy was measured in the pericarp tissue, as described in Bertin et al., 2007. The average value of three measurements per fruit (when allowed for by the fruit's size), was included in the analysis.

In the 2007 experiment, the dynamics of cell number (but not endoreduplication) was measured following the same method as in the 2004 experiment. In addition, cell size distribution (smallest and largest radii and 2D-surface) distributions were measured with ImageJ software (imagej.nih.gov/ij/) in the cell suspension aliquots. About 20 to 25 cells per fruit were measured randomly on different fruits. Cell size distribution were derived for ripe fruits at about 43 days after

anthesis (DAA) for Cervil and 60 DAA for Levovil in the considered growing conditions.

Model description

The model is composed of two interacting modules, both issued from previously published models (Bertin et al., 2007; Fishman and Génard, 1998; Liu et al., 2007). The fruit is described as a collection of cell populations, each one having a specific age, ploidy and volume, which evolve and grow over time during fruit development. The number, age (initiation date) and physiological state (proliferating or endoreduplicating-expanding cells) of each population is predicted by the cell division-endoreduplication module (Bertin et al., 2007), based on genotype-specific parameters. It is assumed that the onset of endoreduplication coincides with the beginning of the expansion phase, i.e. expanding cells are endoreduplicating.

At any time, mass (both fresh and dry component) of expanding cells is computed by a biophysical expansion module according to cell's characteristics (age, ploidy) and depending on available resources and environmental conditions (Fishman and Génard, 1998; Liu et al., 2007). Briefly, cell expansion is described by iteratively solving the Lockhart equation relating the rate of volume increase to the cell's internal pressure and cell's mechanical properties (Lockhart, 1965). Flows of water and solutes across the membrane are described by thermodynamic equations and depend on environmental conditions. The relative importance of each transport process may vary along fruit developmental stages, depending on specific developmental control. A full description of the model and its equations can be found in the section S2 of the Supplemental Material.

In its standard version, the model assumes that all cells have equal access to external resources, independently from the number of cells (no competition). All the parameters of the division- endoreduplication module are considered to be independent from environmental conditions for the time being.

Model initialisation and input

The model starts at the end of the division-only phase, when the proliferative activity of the cells declines and the expansion phase begins (Baldazzi et al., 2013). For Cervil genotype this corresponds to approximatively 8 days before anthesis and to 3 days before anthesis for Levovil genotype (Bertin et al., 2007). The initial number of cells, *n0,* was estimated to 1e4 for the cherry tomato (Cervil) and 1.8e5 for the large-fruited (Levovil) genotype based on a few measurements.

At the beginning of the simulation, all cells are supposed to be proliferating with a ploidy level of 2C (transient ploidy of 4C during cell cycle is not considered). Proliferating cells are supposed to have a constant cell mass, *m0*, as often observed in meristematic cells (homogeneous/uniformity in cell size) (Sablowski and Carnier Dornelas, 2014; Serrano-Mislata et al., 2015). The initial mass of the fruit is therefore Mf(0)*=n0*m0=n0*(w0 +s0),* where *w0* and *s0* are initial cell water and dry mass, respectively. At any time, cells leaving the proliferative phase start to grow, from an initial mass 2**m0* and a ploidy level of *4C,* according to the expansion model and current environmental conditions.

Cell expansion depends on environmental conditions and resources provided by the mother plant. The phloem sugar concentration is assumed to vary daily between 0.15 and 0.35 M whereas stem water potential oscillates between -0.05 and -0.6 MPa i.e. typical pre-dawn and minimal stem water potential measured for the studied genotypes. Temperature and humidity are provided directly by real-time recording of greenhouse climatic conditions.

Choice of the model variants: control of cell expansion capabilities

In the integrated model, a number of time-dependent functions account for developmental regulation of cell's metabolism and physical properties during the

expansion phase (Baldazzi et al. 2013, Liu et al. 2007). Two characteristic time-scales are recognizable in the model: the *cell age,* i.e. the time spent since an individual cell has left the proliferative phase, and *organ age* i.e. the time spent since the beginning of the simulation (Figure 1). Depending on the settings of the corresponding time-dependent functions, different cellular processes may be put under cell-autonomous or non-cell autonomous control (hereafter indicated as organ-wide control), allowing for an *in silico* exploration of alternative control hypotheses in the perspective of the cellular and organismal theories. Moreover, a direct effect of cell DNA content onto cell expansion capabilities may be tested according to biological evidences (Chevalier et al., 2011; Edgar et al., 2014; Sugimoto-Shirasu and Roberts, 2003).

As a default all cellular processes are supposed to be dependent on cell age (cell-autonomous control) with the only exception of cell transpiration which is computed at the organ scale, on the basis of fruit external surface and skin conductance, and then distributed back to individual cells, proportionally to their relative water content (see section S2).

Based on literature information and on preliminary tests ((Baldazzi et al., 2013, 2017), the switch between symplastic and apoplastic transport, σ_p has been selected as the candidate process for an organ-wide control. Indeed, intercellular movement of macromolecules across plasmodesmata has been shown to be restricted by organ age in tobacco leaves (Crawford and Zambryski, 2001; Zambryski, 2004) and it is known to be important for cell-to-cell communication (Han et al., 2013).

The exact mechanisms by which cell DNA content may affect cell expansion remains currently unknown. Based on literature information and common sense, three distinct mechanisms of interaction between endoreduplication and cell expansion were hypothesized.

1) Endoreduplication has been often associated to an elevated protein synthesis

and transcriptional activity (Chevalier et al., 2014) suggesting a general activation of the nuclear and metabolic machinery of the cell to sustain cell growth (Sugimoto-Shirasu and Roberts, 2003). Following these insights, a first hypothesis assumes an effect of endoreduplication on cell expansion as a ploidy-dependent maximal import rate for carbon uptake. For sake of simplicity, the relation was supposed to be linear in the number of endocycles. The corresponding equation, as a function of the cell DNA content (DNAc, being 2 for dividing cells, 4 to 512 for endoreduplicating cells), was

$$v_m = \langle v^0 \rangle * \log_2(DNAc) \quad ,$$

where $\langle v^0 \rangle$ is the average C uptake activity per unit mass.

2) In addition to a high transcriptional activity, endoreduplicating cells are characterized by a reduced surface-to-volume ratio with respect to 2C cells. As a consequence, it is tempting to speculate that one possible advantage of a high ploidy level may reside in a reduction of carbon demand for cell wall and structural units (Barow, 2006; Pirrello et al., 2018). Such an economy may impact cell expansion capabilities in two ways. First, the metabolic machinery could be redirected towards the synthesis of soluble components, thus contributing to the increase of cell's internal pressure and consequent volume expansion.
In the model, the *ssrat* fraction of soluble compound within the cell is developmentally regulated by the age *t* of the cell (Baldazzi et al. 2013) as

$$ssrat = b_{ssrat}\left(1 - e^{-a_{ssrat} * t}\right) + ssrat_0$$

In the presence of a ploidy effect, the final bssrat value was further increased as

$$b_{ssrat} = b^0_{ssrat} * \log_2(DNAc)$$

3) Alternatively, "exceeding" carbon may be used to increase the rate of cell wall synthesis or related proteins, resulting in an increase of cell wall plasticity (Proseus and Boyer, 2006).

In the original expansion model on tomato (Liu et al., 2007) cell wall extensibility

Phi declines during cell maturation (Proseus et al., 1999) as

$$Phi = Phi_{min} + \frac{\left(Phi_{max} - Phi_{min}\right)}{1 + e^{k\left(t - t_0\right)}}$$

In the presence of a ploidy effect, the maximal cell wall extensibility was increased as

$$Phi_{max} = Phi_{max}^{0} * \log_2\left(DNAc\right)$$

The individual and combined effects of organ-wide and ploidy-dependent control (one process at time) on cell expansion were investigated and compared to a full cell-autonomous model. A total of 8 model variants have been tested for each genotype, following the complete experimental design shown in Table 1.

Model calibration

Calibration has been performed using genetic algorithm under R software (library 'genalg'). A two-steps procedure has been used for each tomato genotype.

First, the division-expansion module (7 parameters) was calibrated on data from the 2004 experiment by comparing measured and simulated values of the total cells number and the proportion of cells in different ploidy classes, all along fruit development. The best fitting parameters were selected and kept fixed for the second phase of the calibration, assuming they are independent from environmental conditions.

The expansion module was calibrated on the evolution of pericarp fresh and dry mass from the 2007 experiment, for which cell size distribution were measured. Six parameters have been selected for calibration based on a previous sensitivity analysis (Constantinescu et al., 2016), whereas the others have been fixed to the original models' values (Baldazzi et al., 2013; Fishman and Génard, 1998; Liu et al., 2007). An additional parameter was estimated for model variants M3 to M7 in order to correctly evaluate the strength of the ploidy-dependent control (see

section S3 for more information).

Due to their different structures, the expansion module was calibrated independently for each model variant. The quality of model adjustment was evaluated using a Normalized Root Mean Square Error (NRMSE):

$$NRMSE(x) = 100 \frac{\sqrt{\frac{1}{n}\sum \left(O_i - S_i(x)\right)^2}}{\frac{1}{n}\sum O_i}$$

where Oi and S_i are respectively, the observed and simulated values of pericarp fresh and dry masses, and n is the number of observations. $x = \left(x_{1,} x_2 \ldots x_p\right)$ is parameter set of the evaluated solution. The smaller the NRMSE the better the goodness-of-fit is. A NRMSE < 20% is generally considered good, fair if 20% < NRMSE <30% and poor otherwise.

To avoid high mean fitting errors in each condition, the choice of the best calibration solution was based on a min-max decision criterion (Constantinescu et al., 2016):

$$min_{x \in X}\left\{max\left(NRMSE_{FM}(x), NRMSE_{DM}(x)\right)\right\}$$

where $NRMSE_{FM}$ and $NRMSE_{DM}$ are the normalized root mean square errors for fresh and dry masses respectively. Selected parameters are reported in tables S3 and S4.

Model comparison and selection

On the basis of the best calibration solution, model selection has been performed by comparing measured and simulated cell size distribution, for each model variant. A *semi-quantitive* comparison approach has been used due to the limited experimental information available: the general distribution characteristics (shape, positioning and dispersion) have been characterized rather than a perfect fit. To this aim, 8 descriptive statistical indicators have been computed for each model

variant and compared to those derived from real- data distribution, namely:

- skewness and kurtosis (distribution's shape)
- mean and median cell size (positioning)
- standard deviation (SD) and median absolute deviation (MAD) (data dispersion)
- maximal and minimal cell size (data dispersion)

In order to compare different calibration solutions, a *principal component analysis* (PCA) was performed on the descriptors of cell distribution arising from each model estimation. The ade4 library of R software was used for this purpose (R development Core Team 2006).

RESULTS

A characteristic right-tailed distribution of cell areas

The distribution of cell sizes at a given stage of fruit development directly depends on the particular cell division and expansion patterns followed by the organ up to the considered time. Any change in the cell division or expansion rate will have a consequence on the shape and position of the observed distribution. For both tomato genotypes considered in this study, the cell area distribution at mature stage shows a typical right-tailed shape (Figure 2), compatible with a Weibull or a Gamma distribution (see section S1). The observed cell sizes span up to two orders of magnitude, with cell areas (cross section) ranging from 0.004 to 0.08 $mm^{2,}$ for Cervil genotype, and from 0.005 to 0.28 mm2 for Levovil (Table 3 and 4). The average cell area is calculated to be 0.026 mm2 for the cherry tomato and 0.074 mm2 for the large-fruited genotype, values in agreement with data from other tomato varieties (Bertin, 2005; Renaudin et al., 2017). Data dispersion is higher for the large-fruited genotype, but the shape of the distribution, as measured by its skewness and kurtosis values, is pretty similar for both tomato varieties.

Assuming that cell area distribution is a good descriptor of the underlying interaction patterns among cellular processes, a principal component analysis was performed on 8 statistical descriptors of cell size distribution in order to compare predictions of M0-M7 models (see M&M and Tables 2 and 3). For both genotypes, the two first principal components explained approximately 90% of observed variance and were able to correctly separate models with cell-autonomous control (M0, M5, M6) from models including an organ-wide control of cell expansion (Figure 3 and 4). For Cervil genotype, the intra-model variability of cell size distribution was lower than then inter-model differences, whereas for Levovil models including a ploidy-dependent effect resulted in a similar cell size distribution.

Separation was mainly performed by the first principal component on the basis of the width of the distribution (sd, mad and maximal cell size) and its skewness, both generally increased in models including an interaction between endoreduplication-expansion processes (Figure 3 and 4). Models without organ-wide control are characterized by a reduced dispersion and a larger median value. With respect to experimental data, models combining an organ-wide and a ploidy-dependent control gave the best results.

In the following, the effect of specific control mechanisms on the resulting cell area distribution is analysed in details, based on the results obtained for the best-fitting solution. The corresponding statistical descriptors are reported in Table 2 and 3, for Cervil and Levovil genotype respectively. Note that predicted minimal cell sizes for Levovil genotype are systematically lower than experimental measurements and correspond to the size of proliferating cells. This is partly due to the dissociation method employed for cell counting that underestimates small sub-epidermal cells. These cells although quite numerous contribute little to total pericarp volume and mass (Renaudin et al., 2017).

A simple cell-autonomous control scheme leads to unrealistic cell size distribution

As a benchmark model, the case of a simple cell-autonomous control, without ploidy-dependent effect, was first considered (version M0 of the model). Accordingly, two cells with the same age, even if initiated at different fruit developmental stages, behaved identically in what concerns carbon metabolism, transport and wall mechanical properties. In this scheme, therefore, cell size variations derived exclusively from the dynamics of cell division, which caused a shift in the initiation date for different cohort of cells**.** When applied to our genotypes, the cell-autonomous model was able to reproduce the observed fruit mass dynamics but the corresponding cell size distribution was extremely narrow (Figure 5 A and D), with standard deviation less than 3e-3, and strongly left-tailed (see Table 2 and 3).

Including an organ-wide mechanism that controls cell size (model M1) introduces a source of variance among cells. In this case, two cells of the same age which were initiated at different fruit stages did *not* behave identically, resulting in different expansion capabilities and growth patterns (Baldazzi et al. 2013). Following literature information and preliminary studies (Baldazzi et al., 2017) carbon symplastic transport had been supposed under organ-wide control, via the progressive closure of plasmodesmata with fruit age (Zambryski, 2004) (see M&M section). As a result, the cell size distribution got larger, and skewness increased towards zero values, indicating a symmetric cell size distribution, both for cherry and large-fruited tomatoes. Indeed, the typical right-tail observed in experimental data was absent and the maximum cell size predicted by the model was much smaller than expected. This suggested that a mechanism controlling cell expansion was lacking in the model.

Endoreduplication and cell growth: possible interactions and genotypic effect

A significant correlation between cell size and endoreduplication level has been often reported. However, the molecular mechanism by which ploidy could

modulate cell expansion capabilities remain elusive. In this work, three time-dependent cell properties have been selected as possible targets of ploidy-dependent modulation (see M&M section): *a)* the maximum carbon uptake rate (model version M2), *b)* carbon allocation between soluble and non-soluble compounds (model version M3) *c)* cell wall plasticity (model version M4). The three hypotheses were tested independently on both genotypes, in combination with an organ-wide control. Results are shown in Table 2 and 3. In most cases, the addition of a ploidy effect on cell expansion resulted in a positive skewed distribution, with comparable or increased cell size dispersion and maximum cell size with respect to the M0 and M1 models. The strength of the effect however strongly depended on the genotype, with different ranking among model versions.

For Cervil genotype, a potential control of endoreduplication on both the Vmax (model M2) and cell's allocation strategy (model M3) provided distribution agreement with data, i.e. right-tailed distributions with good dispersion and correct positioning in both mean and median cell area (Figure 5 B and C). The shape of the distribution however was better reproduced by the M2 model, which showed a skewness and kurtosis values close to the observed ones, but the adjustment to fruit growth dynamics, especially for dry mass, was only partially satisfactory (Table 2).
In both models, a high ploidy level resulted in a larger cell size, although the maximum predicted cell size was slightly lower than the observed one. Correlation between ploidy level and cell area was significant with a p-value <0.0001 (Table S5). The heterogeneity of cell sizes usually observed at each ploidy level was correctly captured by the models as a consequence of the asynchrony in cell division and endoreduplication patterns (Bourdon et al., 2011; Roeder et al., 2010). In comparison to the M2 and M3 models, the potential effect of endoreduplication onto cell's mechanical properties (M4) failed to increase cell size variance beyond the values already obtained without any ploidy effect (M1).

For Levovil genotype, the interaction between endoreduplication and expansion

had less impact on the resulting cell distribution. For both model M2 and M4, the addition of a ploidy-dependent effect on cell expansion, although significant, was not able to produce a right-tailed distribution, as observed in experimental data (Figure 5E). The shape of the distribution was pretty symmetric, with skewness values close to zero, reduced dispersion and mean cell size. Only the inclusion of a ploidy-dependent effect on cell's strategy for carbon allocation (model M3) allowed increasing the skewness value up to a reasonable value, but the width of the distribution remained lower than expected with maximal cell sizes not exceeding 0.13 mm2 (against the 0.28mm2 observed) (Figure 5F).

The mechanisms that contribute to cell size variance are likely genotype-dependent

The above results showed that cell distribution can be significantly affected by both an organ-wide control of fruit development and a direct interaction between endoploidy and cell expansion capabilities. In order to better discriminate their respective role, the effect of a ploidy dependent expansion was tested alone, without the contribution of an organ-wide control of cell growth (models M5-M7). Results confirmed that the best results are obtained by a combined action of both an organ-wide control and a ploidy-dependent modulation of cell expansion but the relative importance of the two mechanisms is likely genotype-dependent.

In the case of Levovil, organ-wide control turned out to be a major regulatory mode. Independently of the interactions between endoreduplication and expansion, indeed, models without organ-control (models M5-M7) completely failed to reproduce the observations, resulting in a very narrow and left-tailed cell size distribution (Table 3). Organ-wide coordination of cell expansion appeared to be the main responsible for positive skewness of cell size distribution whereas the addition of an endoreduplication-mediated modulation of cell expansion capabilities, alone, resulted only in a marginal improvement of model's performances.

The relative roles of ploidy-dependent and organ-wide control of cell growth appear more balanced in cherry tomatoes. Indeed, with the exception of model M6, both the organ-wide and the ploidy-mediated control of cell expansion were able to reproduce the expected right-tailed distribution shape (Table 2). However, their concomitant action was needed in order to get a realistic cell size variance. The two mechanisms thus seem to act in synergy to increase cell expansion and final cell size.

A combination of ploidy-dependent control of both carbon uptake and allocation better explains data

In spite of a good agreement with pericarp data, all tested models failed to fully reproduce the observed cell area distribution for Levovil genotype. In particular, the maximum reachable cell size predicted by the models was far lower than the observed data. Up to now, for seek of simplicity, interaction between endoreduplication and expansion has been supposed to affect a single process at time but in reality a combination of effects cannot be excluded. We therefore tried to combine a ploidy-dependent effect on both the maximum carbon uptake and the cell's allocation strategy between soluble and non-soluble compounds (model version M23).

Results showed that, for both genotype, the two mechanisms successfully combined together to improve cell's expansion capabilities. As a consequence, the tail of the distribution straightened and the maximal cell size increased towards realistic values (Figure 6). For Cervil genotype, indeed, the predicted cell size distribution approached the experimental one, as showed by the projection of the M23 model onto the first principal plane (Figure 3). For Levovil genotype, in spite of a significant increase of the maximal cell size, the width of the distribution remained much lower than in experimental data, resulting into a very long-tailed distribution shape.

DISCUSSION

The present paper describes an improved version of an integrated cell division-expansion model that explicitly accounts for DNA endoreduplication, an important mechanism in tomato fruit development. The model is used to investigate the interaction among cell division, endoreduplication and expansion processes, in the framework of the neo-cellular theory (Beemster et al., 2003). To this aim, 8 model variants including or not an organ-wide control of cell development, have been tested and compared to data from two contrasting tomato genotypes. Model simulations showed that a pure cellular control was unable to reproduce the observed cell size distribution in terms of both average cell size and cell variance. In agreement with the neo-cellular theory, the model supported the need for an organ-wide control of cell growth, mediated by cell-to-cell communication via plasmodesmata (Han et al., 2014; Norman et al., 2011) and confirmed the role of endoreduplication as an important modulator of the cell expansion potential.

According to the model, organ-wide control was the main responsible of cell-to-cell variance but a ploidy-mediated effect on cell expansion was needed in order to obtain large cell surface as the ones observed in experimental data. A positive significant correlation between cell size and ploidy level was clearly reproduced, independently of model version, in agreement with recent analysis of cell size in both leaf epidermis (Kawade and Tsukaya, 2017; Roeder et al., 2010) and fruit pericarp (Bourdon et al., 2011).

However, the strength of the correlation may be genotype-dependent. For the cherry tomato variety, our modelling approach showed that a ploidy-dependent control of carbon metabolism (uptake, allocation or a combination of the two), in combination to an organ-wide modulation of cell expansion, was able to generate a cell size distribution close to the observed one. For large-fruited tomato genotype, interaction between endoreduplication and cell expansion via a single process did not suffice to get large cells. Independently of the specific interaction mechanism, the model proved unable to correctly reproduce the observed cell

sizes, resulting in a too narrow and symmetric distribution.
The addition of a double effect of cell's endoploidy on both carbon uptake and allocation was able to increase the maximal cell size close to the correct values, but dispersion remained lower than expected.

Cell stochasticity may be important to explain cell size distribution in fruit

A few reasons may account for the discrepancy observed for the large-fruited variety. A first issue may reside in the quality of experimental data for Levovil genotype. A rapid computation of the average cell size as the pericarp volume over the number of cells at maturity, yields a value significantly lower than the mean of the experimental distribution. This means that the proportion of small cells is underestimated in our dataset, resulting in a distribution that is probably a little flatter and less skewed than the real one.

A second, more fundamental reason of discrepancy is rooted in our modelling approach. Our model is an example of population model: the fruit is described a collection of cell groups, each having specific characteristics in terms of number, mass, age and ploidy level, that dynamically evolve during time. Although asynchrony in the emergence of cell groups allowed to capture a considerable part of cell-to-cell heterogeneity, intrinsic stochasticity of cellular processes (Meyer and Roeder, 2014; Robinson et al., 2011b; Smet and Beeckman, 2011) are not accounted for. Variations in the threshold size for division (often associated to a change in the cell cycle duration) as well as asymmetric cell divisions are considered as important determinant of the final cell size (Dupuy et al., 2010; Osella et al., 2014; Roeder et al., 2010; Stukalin et al., 2013) they may contribute to significantly spread the size distribution of both dividing and expanding cell groups, from the early stages. Moreover, the degree of additional dispersion introduced by cell expansion is likely to depend on the specificity of the underlying mechanisms, with possible interactions with ploidy-dependent and organ-wide controls. Of course, these mechanisms are intrinsic of the development of any new organ, independently of the genotype, but they can

prove more sensitive for Levovil genotype than for Cervil in reason of its higher cell number and longer division windows.

In perspective, the addition of stochastic effects could help to fill the missing variance for both Cervil and Levovil genotypes. To this aim, a novel modelling scheme is needed in which the average cell mass of a group is replaced by a distribution function of cell sizes, whose parameters can evolve with time under the effect of cell expansion processes.

Endoreduplication could regulate cell size through carbon allocation and metabolism

From a biological point of view, the model suggested that endoreduplication may interact with cell's carbon metabolism, increasing the substrate potentially available for cell expansion. This is in line with literature data pointing to ploidy level setting the maximum potential cell size that can be attained or not, depending on internal (hormones) and external (environmental) factors (Breuer et al., 2010; Chevalier et al., 2011; De Veylder et al., 2011). In particular, the model revealed that high ploidy level may increase both the carbon uptake rate and its relative allocation to soluble compounds, thanks to an overall economy in cell wall synthesis (Barow, 2006; Pirrello et al., 2018).

It is important to stress that the molecular basis of the supposed interaction between endoreduplication and expansion are not described in the model and could involve many molecular players. Moreover, the existence of other targets of a ploidy-dependent control cannot be excluded nor the contribution of other mechanisms to the control of the final cell size. In many fruit species including tomato, a negative correlation between average cell size and cell number has been observed, suggesting the existence of a competition for resources (Lescourret and Génard, 2003; Prudent et al., 2013). This kind of mechanism may contribute to broaden the range of attainable cell sizes, increasing size variance among first and late-initiated cells (see section S5).The importance of such an effect may vary with genotype and environmental conditions (Bertin,

2005; Quilot and Génard, 2008). This may be especially important for large-fruited tomatoes for which cell number is large.

Measurement of cell size distribution: promises and challenges to understand the control of fruit growth

Further work is needed in order to identify the mechanisms behind organ growth and cell size determination. To this aim, the analysis of cell size distribution shows up as a promising approach. When looking at our results, indeed, the NRMSE with respect to pericarp fresh and dry mass was always between 20% and 30% indicating a satisfactory agreement with data, independently from the model version and the tomato genotype. This highlights the fact that the dynamics of fruit growth alone is not enough to discriminate between several biologically-plausible models. In this sense, cell size distribution represents a much more informative dataset as it uniquely results from the specific cell division and expansion patterns of the organ (Halter et al., 2009).

The assessment of cell sizes in an organ is not an easy task though. As illustrated by the case of Levovil, the employed measurement technique may have important consequences on the resulting cell size distribution (Legland et al., 2012). Indeed, mechanical constraints acting on real tissues as well as vascularisation can largely modify cell shape, resulting in elongated or multi-lobed cells (Ivakov and Persson, 2013). Thus, if the orientation of 2D slices can potentially affect the resulting cell area estimation, possible differences between *in-vivo* tissues and dissociated cells, both in number and size, should also be checked.

The use of mutant or modified strains (Musseau et al., 2017) in combination with recent advancements in microscopy and tomography (Mebatsion et al., 2009; Wuyts et al., 2010) could now permit the acquisition of more reliable datasets, opening the way to an in-depth investigation of cell size variance in relation to the their position within the fruit (Renaudin et al., 2017) and to the underlying molecular processes. At term, improvements in the ability of computation models

to integrate the multiple facets of organ development in a mechanistic way can help to evaluate and quantify the contribution of the different processes to the control of cell growth.

Acknowledgments

The authors warmly thank B. Brunel for help with cell measurements. The authors are grateful to Inria Sophia Antipolis – Méditerranée "NEF" computation cluster for providing resources and support. This work was partially funded by the Agence Nationale de la Recherche, Project “Frimouss” (grant no. ANR–15–CE20–0009) and by the Agropolis Foundation under the reference ID 1403-032 through the « Investissements d’avenir » programme (Labex Agro:ANR-10-LABX-0001-01).

Literature cited

Asl, L.K., Dhondt, S., Boudolf, V., Beemster, G.T.S., Beeckman, T., Inzé, D., Govaerts, W., and De Veylder, L. (2011). Model-based analysis of Arabidopsis leaf epidermal cells reveals distinct division and expansion patterns for pavement and guard cells. Plant Physiol. *156*, 2172–2183.

Baldazzi, V., Bertin, N., Genard, M., and Génard, M. (2012). A model of fruit growth integrating cell division and expansion processes. In Acta Horticulturae, (International Society for Horticultural Science (ISHS); Leuven; Belgium), pp. 191–196.

Baldazzi, V., Pinet, A., Vercambre, G., Bénard, C., Biais, B., and Génard, M. (2013). In-silico analysis of water and carbon relations under stress conditions. A multi-scale perspective centered on fruit. Front. Plant Sci. *4*, 495.

Baldazzi, V., Génard, M., and Bertin, N. (2017). Cell division, endoreduplication and expansion processes: setting the cell and organ control into an integrated model of tomato fruit development. Acta Hortic. *1182*.

Barow, M. (2006). Endopolyploidy in seed plants. BioEssays *28*, 271–281.

Beemster, G.T.S., Fiorani, F., and Inzé, D. (2003). Cell cycle: the key to plant growth control? Trends Plant Sci. *8*, 154–158.

Bertin, N. (2005). Analysis of the tomato fruit growth response to temperature and plant fruit load in relation to cell division, cell expansion and DNA endoreduplication. Ann. Bot. *95*, 439–447.

Bertin, N., Génard, M., and Fishman, S. (2003). A model for an early stage of tomato fruit development: cell multiplication and cessation of the cell proliferative activity. Ann. Bot. *92*, 65–72.

Bertin, N., Lecomte, A., Brunel, B., Fishman, S., and Génard, M. (2007). A model describing cell polyploidization in tissues of growing fruit as related to cessation of cell proliferation. J. Exp. Bot. *58*, 1903–1913.

Boudon, F., Chopard, J., Ali, O., Gilles, B., Hamant, O., Boudaoud, A., Traas, J., and Godin, C. (2015). A Computational Framework for 3D Mechanical Modeling of Plant Morphogenesis with Cellular Resolution. PLoS Comput. Biol. *11*, e1003950.

Bourdon, M., Coriton, O., Pirrello, J., Cheniclet, C., Brown, S.C., Poujol, C., Chevalier, C., Renaudin, J.-P.P., and Frangne, N. (2011). In planta quantification of endoreduplication using fluorescent in situ hybridization (FISH). Plant J. *66*, 1089–1099.

Breuer, C., Ishida, T., and Sugimoto, K. (2010). Developmental control of endocycles and cell growth in plants. Curr. Opin. Plant Biol. *13*, 654–660.

Bünger-Kibler, S., and Bangerth, F. (1982). Relationship between cell number, cell size and fruit size of seeded fruits of tomato (Lycopersicon esculentum Mill.), and those induced parthenocarpically by the application of plant growth regulators. Plant Growth Regul. *1*, 143–154.

Chevalier, C., Nafati, M., Mathieu-Rivet, E., Bourdon, M., Frangne, N., Cheniclet, C., Renaudin, J.-P., Gévaudant, F., and Hernould, M. (2011). Elucidating the functional role of endoreduplication in tomato fruit development. Ann. Bot. *107*, 1159–1169.

Chevalier, C., Bourdon, M., Pirrello, J., Cheniclet, C., Gevaudant, F., Frangne, N., Gévaudant, F., and Frangne, N. (2014). Endoreduplication and fruit growth in tomato: evidence in favour of the karyoplasmic ratio theory. J. Exp. Bot. *65*, 1–16.

Constantinescu, D., Memmah, M.-M., Vercambre, G., Génard, M., Baldazzi, V.,

731Causse, M., Albert, E., Brunel, B., Valsesia, P., and Bertin, N. (2016). Model-
732Assisted Estimation of the Genetic Variability in Physiological Parameters Related
733to Tomato Fruit Growth under Contrasted Water Conditions. Front. Plant Sci. *7*,
7341–17.

735Crawford, K.M., and Zambryski, P.C. (2001). Non-targeted and targeted protein
736movement through plasmodesmata in leaves in different developmental and
737physiological states. Plant Physiol. *125*, 1802–1812.

738Dupuy, L., Mackenzie, J., and Haseloff, J. (2010). Coordination of plant cell
739division and expansion in a simple morphogenetic system. Proc. Natl. Acad. Sci.
740U. S. A. *107*, 2711–2716.

741Edgar, B.A., Zielke, N., and Gutierrez, C. (2014). Endocycles: a recurrent
742evolutionary innovation for post-mitotic cell growth. Nat. Rev. Mol. Cell Biol. *15*,
743197–210.

744Fanwoua, J., De Visser, P.H.B., Heuvelink, E., Yin, X., Struik, P.C., and Marcelis,
745L.F.M. (2013). A dynamic model of tomato fruit growth integrating cell division, cell
746growth and endoreduplication. Funct. Plant Biol. *40*, 1098.

747Ferjani, A., Horiguchi, G., Yano, S., and Tsukaya, H. (2007). Analysis of leaf
748development in fugu mutants of Arabidopsis reveals three compensation modes
749that modulate cell expansion in determinate organs. Plant Physiol. *144*, 988–999.

750Fishman, S., and Génard, M. (1998). A biophysical model of fruit growth:
751simulation of seasonal and diurnal dynamics of mass. Plant Cell Env. *21*, 739–
752752.

753Fleming, A.J. (2006). The integration of cell proliferation and growth in leaf
754morphogenesis. J. Plant Res. *119*, 31–36.

755Halter, M., Elliott, J.T., Hubbard, J.B., Tona, A., and Plant, A.L. (2009). Cell
756volume distributions reveal cell growth rates and division times. J. Theor. Biol.
757*257*, 124–130.

758Han, X., Kumar, D., Chen, H., Wu, S., and Kim, J.-Y. (2013). Transcription factor-
759mediated cell-to-cell signalling in plants. J. Exp. Bot.

760Han, X., Kumar, D., Chen, H., Wu, S., and Kim, J.Y. (2014). Transcription factor-
761mediated cell-to-cell signalling in plants. J. Exp. Bot. *65*, 1737–1749.

762Horiguchi, G., and Tsukaya, H. (2011). Organ Size Regulation in Plants: Insights
763from Compensation. Front. Plant Sci. *2*, 24.

Ivakov, A., and Persson, S. (2013). Plant cell shape: modulators and measurements. Front. Plant Sci. *4*, 439.

John, P.C.L., and Qi, R. (2008). Cell division and endoreduplication: doubtful engines of vegetative growth. Trends Plant Sci. *13*, 121–127.

Kawade, K., and Tsukaya, H. (2017). Probing the stochastic property of endoreduplication in cell size determination of Arabidopsis thaliana leaf epidermal tissue. PLoS One *12*, e0185050.

Kawade, K., Horiguchi, G., and Tsukaya, H. (2010). Non-cell-autonomously coordinated organ size regulation in leaf development. Development *137*, 4221–4227.

Kuchen, E.E., Fox, S., de Reuille, P.B., Kennaway, R., Bensmihen, S., Avondo, J., Calder, G.M., Southam, P., Robinson, S., Bangham, A., et al. (2012). Generation of leaf shape through early patterns of growth and tissue polarity. Science *335*, 1092–1096.

Lee, H.-C., Chen, Y.-J., Markhart, A.H., and Lin, T.-Y. (2007). Temperature effects on systemic endoreduplication in orchid during floral development. Plant Sci. *172*, 588–595.

Legland, D., Devaux, M.-F., Bouchet, B., Guillon, F., and Lahaye, M. (2012). Cartography of cell morphology in tomato pericarp at the fruit scale. J. Microsc. *247*, 78–93.

Lescourret, F., and Génard, M. (2003). A multi-level theory of competition for resources applied to fruit production. Écoscience *10*, 334–341.

Liu, H.-F.F.H.-F., Génard, M., Guichard, S., and Bertin, N. (2007). Model-assisted analysis of tomato fruit growth in relation to carbon and water fluxes. J. Exp. Bot. *58*, 3567–3580.

Löfke, C., Dünser, K., Scheuring, D., Kleine-Vehn, J., Barbez, E., Kubeš, M., Rolčík, J., Béziat, C., Pěnčík, A., Wang, B., et al. (2015). Auxin regulates SNARE-dependent vacuolar morphology restricting cell size. Elife *4*, 119–122.

Lucas, M., Kenobi, K., von Wangenheim, D., Voβ, U., Swarup, K., De Smet, I., Van Damme, D., Lawrence, T., Péret, B., Moscardi, E., et al. (2013). Lateral root morphogenesis is dependent on the mechanical properties of the overlaying tissues. Proc. Natl. Acad. Sci. U. S. A. *110*, 5229–5234.

Mebatsion, H.K., Verboven, P., Melese Endalew, A., Billen, J., Ho, Q.T., and

Nicolaï, B.M. (2009). A novel method for 3-D microstructure modeling of pome fruit tissue using synchrotron radiation tomography images. J. Food Eng. *93*, 141–148.

Melaragno, J., Mehrotra, B., and Coleman, A. (1993). Relationship between endopolyploidy and cell size in epidermal tissue of Arabidopsis. Plant Cell Online *5*, 1661–1668.

Musseau, C., Just, D., Jorly, J., G?vaudant, F., Moing, A., Chevalier, C., Lemaire-Chamley, M., Rothan, C., and Fernandez, L. (2017). Identification of Two New Mechanisms That Regulate Fruit Growth by Cell Expansion in Tomato. Front. Plant Sci. *8*, 1–15.

Norman, J.M. Van, Breakfield, N.W., Benfey, P.N., Carolina, N., Van Norman, J.M., Breakfield, N.W., and Benfey, P.N. (2011). Intercellular communication during plant development. Plant Cell *23*, 855–864.

Okello, R.C.O., Heuvelink, E., de Visser, P.H.B., Struik, P.C., and Marcelis, L.F.M. (2015). What drives fruit growth? Funct. Plant Biol. *42*, 817.

Osella, M., Nugent, E., and Cosentino Lagomarsino, M. (2014). Concerted control of Escherichia coli cell division. Proc. Natl. Acad. Sci. U. S. A. *111*, 4–8.

Pirrello, J., Deluche, C., Frangne, N., Gévaudant, F., Maza, E., Djari, A., Bourge, M., Renaudin, J.-P., Brown, S., Bowler, C., et al. (2018). Transcriptome profiling of sorted endoreduplicated nuclei from tomato fruits: how the global shift in expression ascribed to DNA ploidy influences RNA-Seq data normalization and interpretation. Plant J. *93*, 387–398.

Proseus, T.E., and Boyer, J.S. (2006). Identifying cytoplasmic input to the cell wall of growing Chara corallina. J. Exp. Bot. *57*, 3231–3242.

Proseus, T.E., Ortega, J.K.E., and Boyer, J.S. (1999). Separating Growth from Elastic Deformation during Cell Enlargement. Plant Physiol. *119*, 775–784.

Prudent, M., Dai, Z.W., Génard, M., Bertin, N., Causse, M., and Vivin, P. (2013). Resource competition modulates the seed number-fruit size relationship in a genotype-dependent manner: A modeling approach in grape and tomato. Ecol. Modell.

Quilot, B., and Génard, M. (2008). Is competition between mesocarp cells of peach fruits affected by the percentage of wild species (Prunus davidiana) genome? J. Plant Res. *121*, 55–63.

Renaudin, J.-P., Deluche, C., Cheniclet, C., Chevalier, C., and Frangne, N. (2017). Cell layer-specific patterns of cell division and cell expansion during fruit set and fruit growth in tomato pericarp. J. Exp. Bot. *68*, 1613–1623.

Rewers, M., Sadowski, J., and Sliwinska, E. (2009). Endoreduplication in cucumber (Cucumis sativus) seeds during development, after processing and storage, and during germination. Ann. Appl. Biol. *155*, 431–438.

Robinson, S., Barbier de Reuille, P., Chan, J., Bergmann, D., Prusinkiewicz, P., and Coen, E. (2011). Generation of spatial patterns through cell polarity switching. Science (80-.). *333*, 1436–1440.

Roeder, A.H.K., Chickarmane, V., Cunha, A., Obara, B., Manjunath, B.S., and Meyerowitz, E.M. (2010). Variability in the control of cell division underlies sepal epidermal patterning in Arabidopsis thaliana. PLoS Biol. *8*, e1000367.

Sablowski, R., and Carnier Dornelas, M. (2014). Interplay between cell growth and cell cycle in plants. J. Exp. Bot. *65*, 2703–2714.

Serrano-Mislata, A., Schiessl, K., and Sablowski, R. (2015). Active Control of Cell Size Generates Spatial Detail during Plant Organogenesis. Curr. Biol. *25*, 2991–2996.

Stukalin, E.B., Aifuwa, I., Kim, J.S., Wirtz, D., and Sun, S.X. (2013). Age-dependent stochastic models for understanding population fluctuations in continuously cultured cells. J. R. Soc. Interface *10*, 20130325.

Sugimoto-Shirasu, K., and Roberts, K. (2003). “Big it up”: endoreduplication and cell-size control in plants. Curr. Opin. Plant Biol. *6*, 544–553.

Tsukaya, H. (2003). Organ shape and size: a lesson from studies of leaf morphogenesis. Curr. Opin. Plant Biol. *6*, 57–62.

De Veylder, L., Larkin, J.C., and Schnittger, A. (2011). Molecular control and function of endoreplication in development and physiology. Trends Plant Sci. *16*, 624–634.

von Wangenheim, D., Fangerau, J., Schmitz, A., Smith, R.S., Leitte, H., Stelzer, E.H.K., and Maizel, A. (2016). Rules and Self-Organizing Properties of Post-embryonic Plant Organ Cell Division Patterns. Curr. Biol. *26*, 439–449.

Wuyts, N., Palauqui, J.-C., Conejero, G., Verdeil, J.-L., Granier, C., and Massonnet, C. (2010). High-contrast three-dimensional imaging of the Arabidopsis leaf enables the analysis of cell dimensions in the epidermis and

mesophyll. Plant Methods *6*, 17.

Zambryski, P.C. (2004). Cell-to-cell transport of proteins and fluorescent tracers via plasmodesmata during plant development. J. Cell Biol. *164*, 165–168.

Figures

Figure 1*:* Scheme of the integrated model. The fruit is described as a collection of cell populations, each one having a specific age, ploidy and volume. Cells can be either proliferating or expanding-endoreduplicating. The number of cells in each class is predicted by the division-endoreduplication module, assuming a progressive decline of cells' proliferating activity. Expanding cells grow according to the expansion module which provides a biophysical description of the main processes involved in carbon and water accumulation. It is assumed that the onset of endoreduplication coincides with the beginning of the expansion phase. Two timescales are recognizable in the model: the organ age i.e. the time since the beginning of the simulation, and the cell age i.e. the time since the cell left the mitotic cycle and entered the expansion-endoreduplication phase. Depending on the model version, cell expansion may be modulated by organ age (organ-wide control) and/or by cell's ploidy.

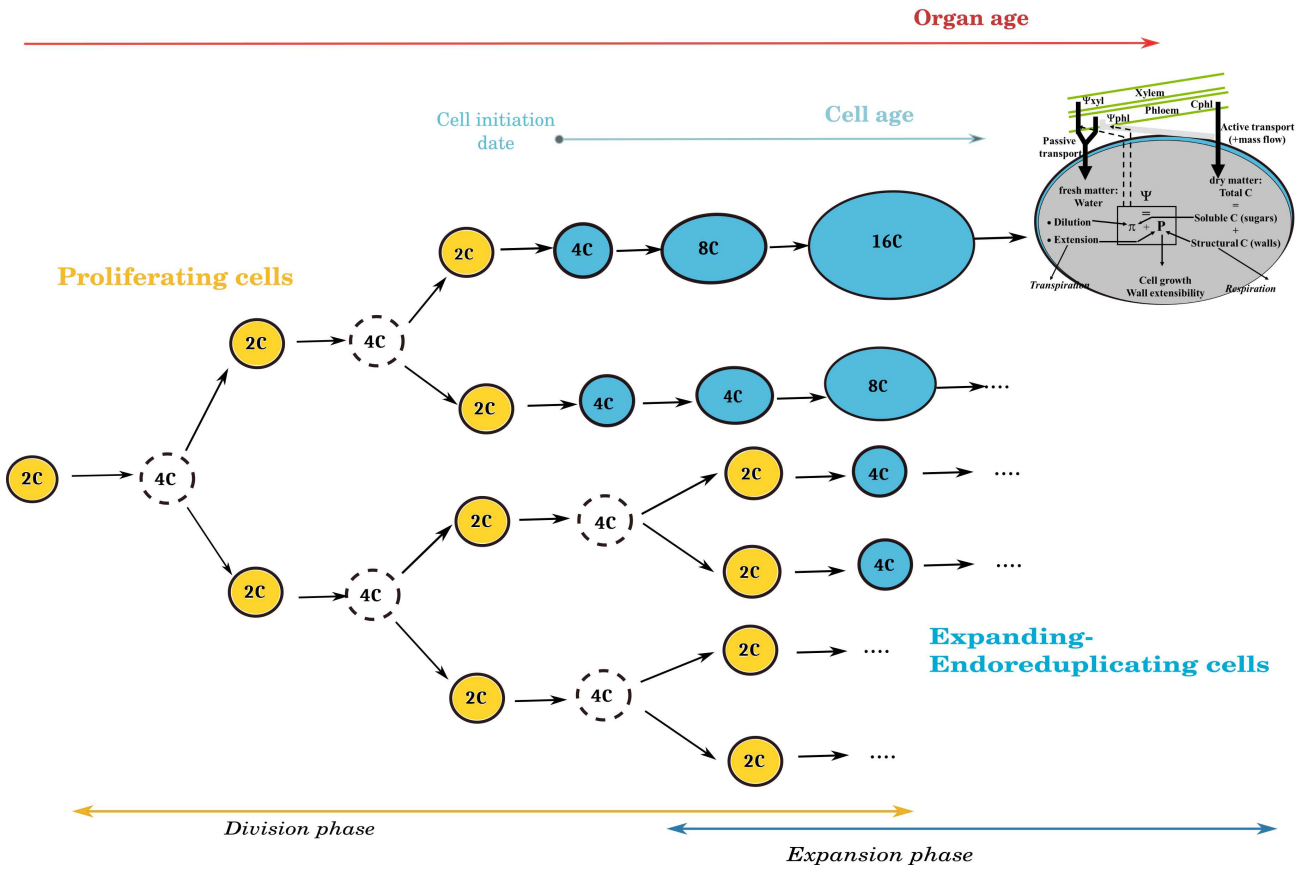

906

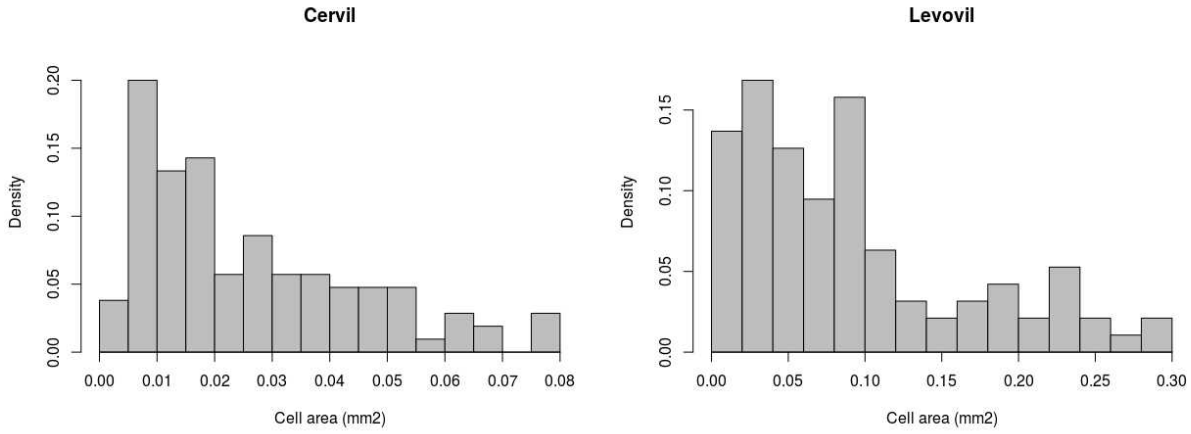

908Figure 2**:** Measured cell size distribution at fruit maturity Left: Cervil genotype. Right: Levovil
909genotype.
910
911
912
913

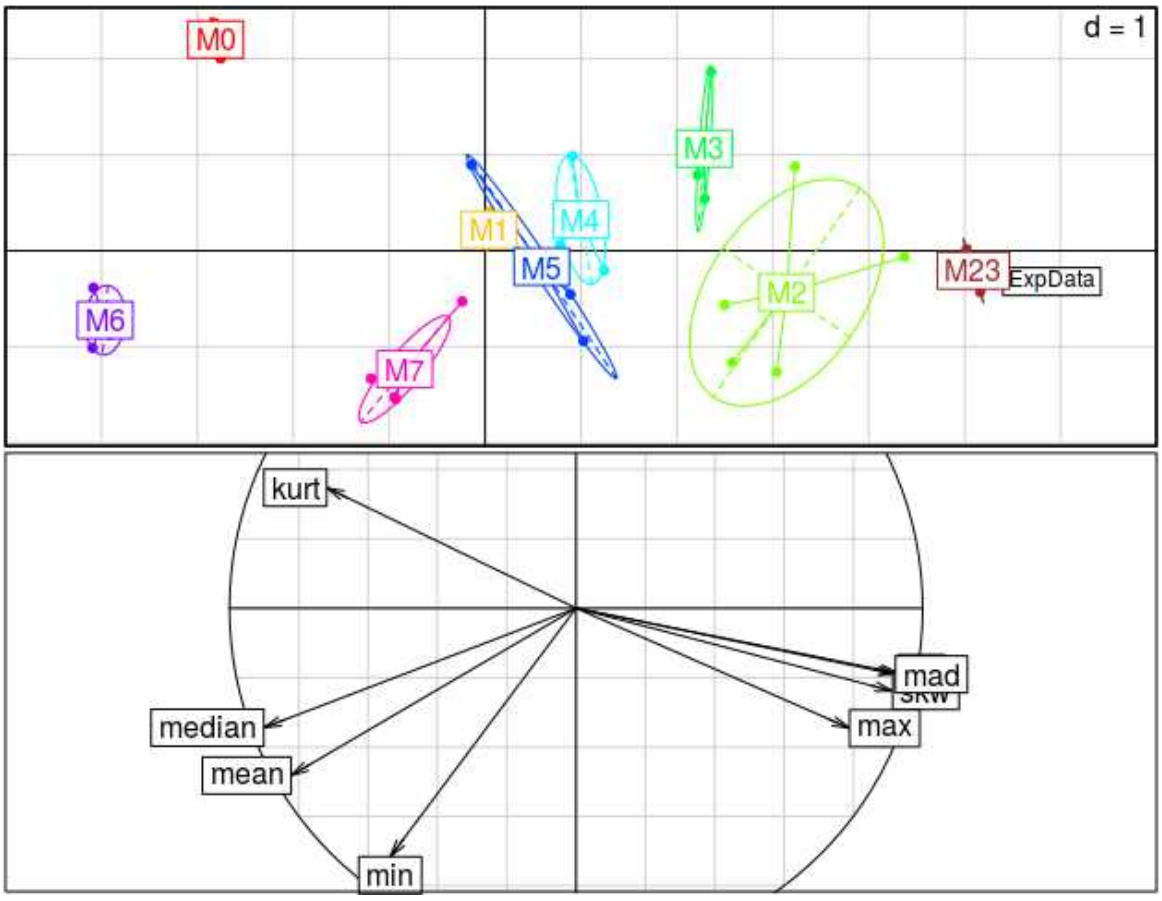
d = 1
M0
M1
M2
M3
M4
M5
M6
M7
M23
ExpData
kurt
mad
median
max
mean
min

Figure 3: Principal component analysis (PCA) cell size distributions obtained for the different estimations of models M0-M7 on Cervil genotype. 8 statistical descriptors are used as variables to characterize cell distribution. Measured cell size distribution results of model M23 are projected as a supplementary observation. *Top:* Projection of individual distributions on the PC1-PC2 plane. Model variants are tagged with different colors. *Bottom:* Correlation of the variables with the first two principal components.

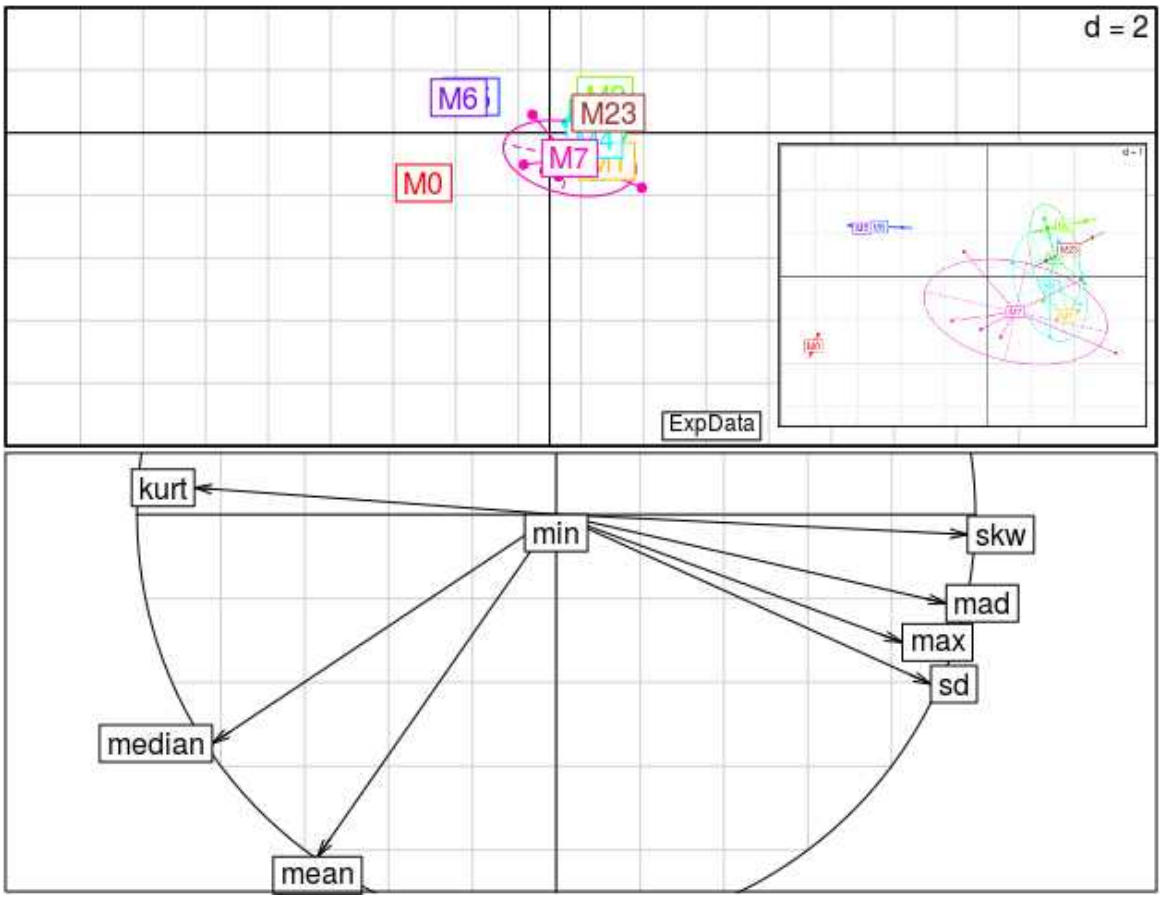

Figure 4: Principal component analysis (PCA) cell size distributions obtained for the different estimations of models M0-M7 on Levovil genotype. 8 statistical descriptors are used as variables to characterize cell distribution. Measured cell size distribution and results of model M23 are projected as a supplementary observation. *Top:* Projection of individual distributions on the PC1-PC2 plane. Model variants are tagged with different colors. *Bottom:* Correlation of the variables with the first two principal components.

Figure 5: Predicted cell area distribution at fruit maturity. On the left side, Cervil genotype: A: model M0, B: model M2, C: model M3. On the right side, Levovil genotype: D: model M0, E: modelM2, F: model M3.

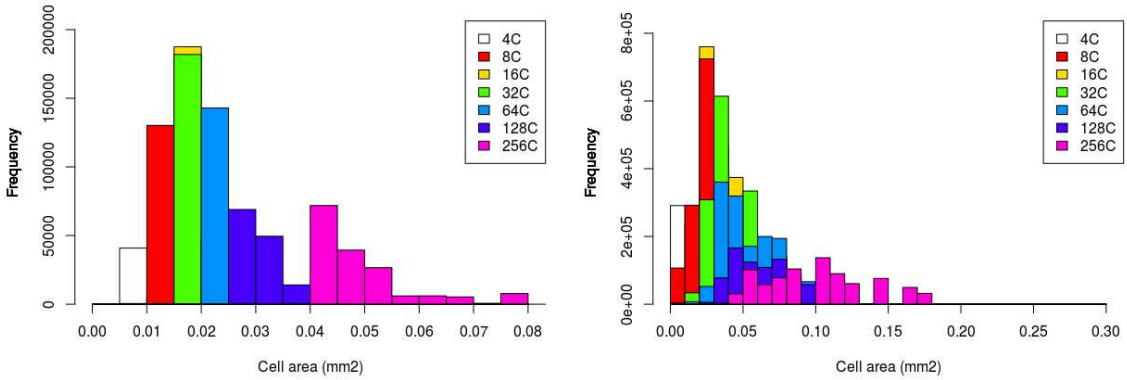

Figure 6: Predicted cell area distribution at fruit maturity for model M23, combining a ploidy-dependent effect on both carbon uptake and allocation. Left: Cervil genotype. Right: Levovil genotype.

Tables

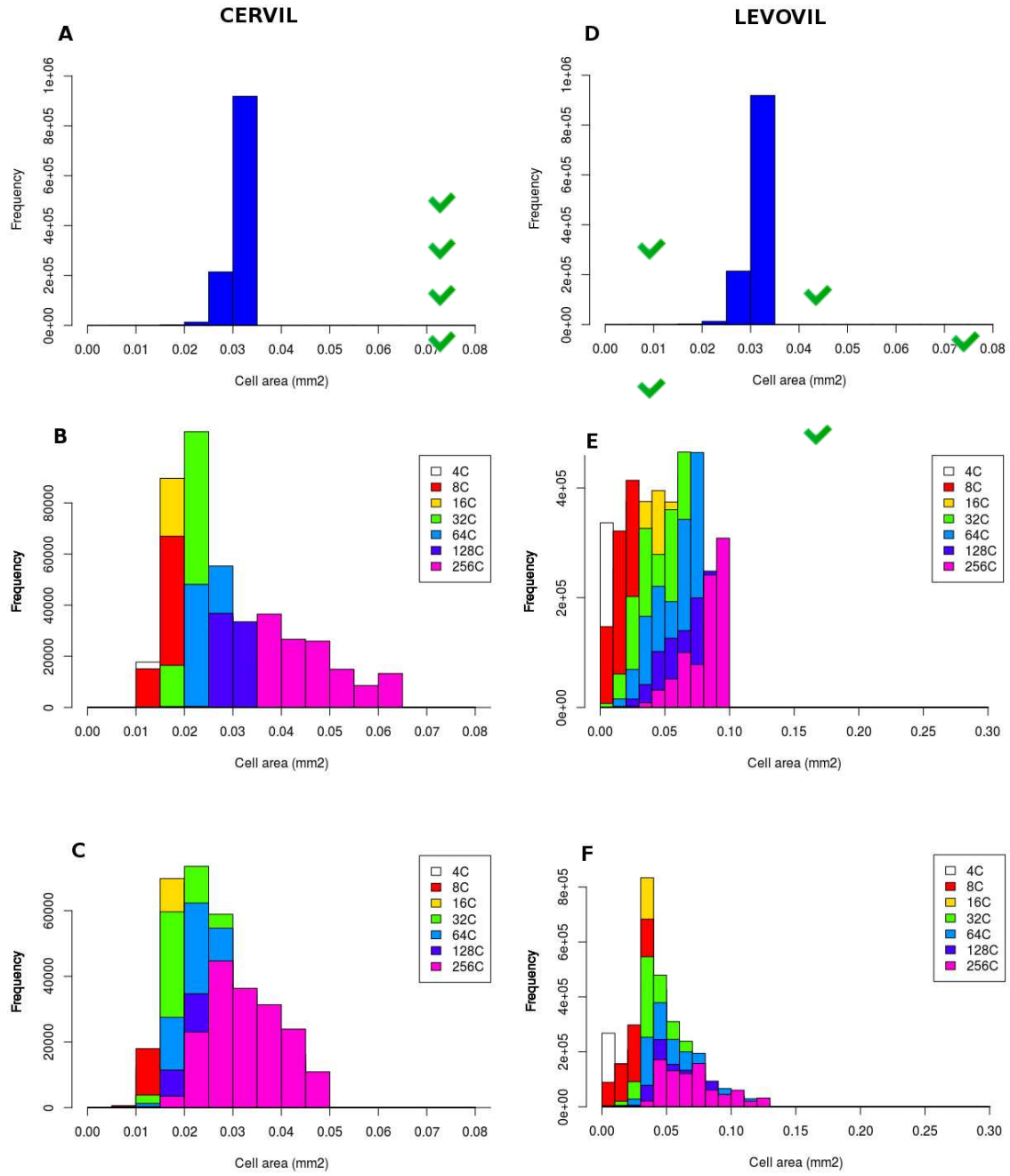

Table 1: Experimental design showing the characteristics of the 8 model versions tested in the paper.

MODEL	FRUIT MASS		CELL DISTRIBUTION							
	FIT QUALITY		**SHAPE**		**POSITIONING**				**DISPERSION**	
	NRMSE FM	NRMSE DM	Skewness	Kurtosis	Mean	Median	Min	Max	SD	MAD
Exp Data			**0.97**	**3.13**	**0.026**	**0.019**	**0.0039**	**0.08**	**0.019**	**0.016**
M0	31.49	31.34	-4.06	30.34	0.030	0.031	0.0042	0.033	0.0015	0.0005
M1	28.32	29.58	0.42	3.07	0.030	0.029	0.0044	0.041	0.0046	0.0042
M2	23	36	0.98	3.58	0.027	0.025	0.0035	0.062	0.011	0.0099
M3	20.18	31.24	0.53	2.58	0.026	0.025	0.0033	0.046	0.0077	0.008
M4	24.97	27.73	0.53	3.45	0.027	0.027	0.0040	0.045	0.005	0.005
M5	34.35	37.02	0.33	3.44	0.029	0.029	0.0040	0.037	0.0035	0.003
M6	34.21	33.81	-3.7	24.9	0.036	0.036	0.0051	0.039	0.002	0.0008
M7	29.53	32.47	0.24	3.34	0.034	0.033	0.0040	0.056	0.005	0.005
M23	23.33	33.05	2.0	8.9	0.026	0.021	0.0037	0.11	0.015	0.009

Table 2 Statistical descriptors for the measured and predicted cell area distribution for Cervil genotype. The NRMSE scores for predicted pericarp dry and fresh masses corresponding to the selected solution are reported under the columns “Fit Quality”. For an easier interpretation, green boxes indicate an agreement within 30% with respect to experimental data, yellow an agreement between 30 and 40%, white between 40% and 70% and red a strong discrepancy (over 70% difference with respect to data).

MODEL	FRUIT MASS		CELL DISTRIBUTION							
	FIT QUALITY		**SHAPE**		**POSITIONING**				**DISPERSION**	
	NRMSE FM	NRMSE DM	Skewness	Kurtosis	Mean	Median	Min	Max	SD	MAD
Exp Data			**0.99**	**3.01**	**0.092**	**0.074**	**0.0048**	**0.28**	**0.075**	**0.063**
M0	23.3	25.27	-2.37	7.89	0.069	0.077	0.00049	0.078	0.017	0.0023
M1	25.79	25.32	0.26	2.13	0.059	0.052	0.00049	0.12	0.030	0.034
M2	25.39	25.59	-0.075	2.2	0.047	0.043	0.00049	0.12	0.022	0.017
M3	25.77	25.01	0.67	3.74	0.047	0.043	0.00049	0.13	0.022	0.017
M4	23.64	25.23	-0.15	2.8	0.053	0.054	0.00049	0.11	0.022	0.020
M5	23.36	27.47	-1.51	5.85	0.054	0.056	0.00049	0.077	0.014	0.008
M6	23.61	25.15	-2.22	7.31	0.055	0.060	0.00049	0.066	0.013	0.004
M7	23.74	25.42	-0.56	3.41	0.063	0.066	0.00049	0.10	0.020	0.018
M23	25.45	28.20	1.46	5.73	0.047	0.039	0.00049	0.018	0.028	0.021

Table 3: Statistical descriptors for the measured and predicted cell area distribution for Levovil genotype. The NRMSE scores for predicted pericarp dry and fresh masses corresponding to the selected solution are reported under the columns “Fit Quality”. For an easier interpretation, green boxes indicate an agreement within 30% with respect to experimental data, yellow an agreement between 30 and 40%, white between 40% and 70% and red a strong discrepancy (over 70% difference with respect to data).